SPANDIDOS PUBLICATIONS

INTERNATIONAL JOURNAL OF ONCOLOGY 55: 81-92, 2019

PLEKHO1 knockdown inhibits RCC cell viability *in vitro* and *in vivo*, potentially by the Hippo and MAPK/JNK pathways

ZI YU[1,2*], QIANG LI[3*], GEJUN ZHANG[2], CHENGCHENG LV[1], QINGZHUO DONG[2], CHENG FU[1], CHUIZE KONG[2] and YU ZENG[1]

[1]Department of Urology, Cancer Hospital of China Medical University, Liaoning Cancer Hospital and Institute, Shenyang, Liaoning 110042; [2]Department of Urology, The First Hospital of China Medical University, Shenyang, Liaoning 110001; [3]Department of Pathology, Cancer Hospital of China Medical University, Liaoning Cancer Hospital and Institute, Shenyang, Liaoning 110042, P.R. China

Received November 17, 2018; Accepted May 17, 2019

DOI: 10.3892/ijo.2019.4819

Abstract. Renal cell carcinoma (RCC) is the most common type of kidney cancer. By analysing The Cancer Genome Atlas (TCGA) database, 16 genes were identified to be consistently highly expressed in RCC tissues compared with the matched para-tumour tissues. Using a high-throughput cell viability screening method, it was found that downregulation of only two genes significantly inhibited the viability of 786-O cells. Among the two genes, pleckstrin homology domain containing O1 (PLEKHO1) has never been studied in RCC, to the best of our knowledge, and its expression level was shown to be associated with the prognosis of patients with RCC in TCGA dataset. The upregulation of PLEKHO1 in RCC was first confirmed in 30 paired tumour and para-tumour tissues. Then, the effect of PLEKHO1 on cell proliferation and apoptosis was assessed *in vitro*. Additionally, xenograft tumour models were established to investigate the function of PLEKHO1 *in vivo*. The results showed that PLEKHO1 knockdown significantly inhibited cell viability and facilitated apoptosis *in vitro* and impaired tumour formation *in vivo*. Thus, PLEKHO1 is likely to be associated with the viability of RCC cells *in vitro* and *in vivo*. Further gene expression microarray and co-expression analyses showed that PLEKHO1 may be involved in the serine/threonine-protein kinase hippo and JNK signalling pathways. Together, the results of the present study suggest that PLEKHO1 may contribute to the development of RCC, and therefore, further study is needed to explore its potential as a therapeutic target.

Correspondence to: Professor Yu Zeng, Department of Urology, Cancer Hospital of China Medical University, Liaoning Cancer Hospital and Institute, 44 Xiaoheyan Road, Shenyang, Liaoning 110042, P.R. China
E-mail: zengyud@hotmail.com

Professor Chuize Kong, Department of Urology, The First Hospital of China Medical University, 155 Nanjing North Street, Shenyang, Liaoning 110001, P.R. China
E-mail: kongchuizecmu@163.com

*Contributed equally

Key words: cell proliferation, Hippo pathway, JNK pathway, PLEKHO1 protein, renal cell carcinoma

Introduction

In 2018, kidney cancer is estimated to be diagnosed in nearly 403,200 people worldwide and to lead to almost 175,000 cancer-related deaths according to the latest data released by the International Agency for Research on Cancer (1). The course of kidney cancer is commonly palliative and uneventful without initial distinct clinical symptoms and signs (2). Hence, patients fail to be diagnosed at the early stage of cancer. For localized tumours, surgical excision by partial nephrectomy or radical nephrectomy is now recognized as the preferred choice of treatment, while for the patients who present with metastatic or unresectable tumours, systemic treatment is needed (3). Unfortunately, renal cell carcinoma (RCC), especially clear cell (cc)RCC, which accounts for up to 90% of all kidney cancers, originates from the proximal convoluted tubule, which highly expresses multidrug resistant protein-1, resulting in the high resistance of RCC to chemotherapy (4). Although the development of drugs targeting neovascularization or mammalian target of rapamycin (mTOR) improves the survival of RCC patients, drug resistance inevitably develops (5). Recently, checkpoint immunotherapy has shown promise; however, the complete response rate still remains at a low level (6). Therefore, it is imperative that insight into the mechanisms underlying the development of RCC is gained and that novel therapeutic targets to improve the prognosis of RCC are identified.

The Cancer Genome Atlas (TCGA) was launched in 2005 with the aim of categorizing all genetic alterations contributing to cancer formation and development to explore new clinical therapies as well as diagnostic and preventive strategies. By 2015, over 30 human tumour types had been incorporated into the database, including RCC (7). By analysing the RCC gene expression data in TCGA database and then performing a high-throughput cell viability screening, the authors found

that pleckstrin homology domain-containing family O member 1 (PLEKHO1) was aberrantly expressed in tumour tissue and probably contributed to tumour growth. PLEKHO1 [also known as casein kinase (CK)2-interacting protein 1] was originally identified as a novel CK2-binding protein and has been shown to mediate the specific function of CK2 by sequestering or recruiting CK2 to the plasma membrane (8-10). The PLEKHO1 protein possesses multiple active sites, including a pleckstrin homology domain at the N-terminus, a putative leucine zipper (LZ) motif at the C-terminus and five proline-rich motifs throughout the protein, which mediate diverse protein-protein interactions (11).

On the basis of its structural characteristics, PLEKHO1 was implicated in different signalling pathways involved in diverse biological processes, such as cell proliferation (9,12), cell apoptosis (13), cell differentiation (9), cell morphology (14,15), macrophage migration/proliferation (16,17) and protein metabolism (18,19). Recently, it was found that PLEKHO2, which belongs to the same superfamily as PLEKHO1, is a key factor for macrophage survival (20). Lu *et al* (18) reported that the expression of PLEKHO1 negatively regulated bone formation, and after that study, the 6-liposome system (AspSerSer) was developed to guide PLEKHO1 small interfering (si) RNAs to bone formation surfaces to treat osteoporosis (21). In addition, other studies have demonstrated that PLEKHO1 plays roles in many diseases in humans and animal models, such as cancer (22-24), diabetic nephropathy (25), fatty liver disease (26) and chronic heart failure (27). All these findings suggest the potential significance of PLEKHO1 in both biological and pathological processes of the human body. Nevertheless, the functional roles and detailed mechanisms of PLEKHO1 in diseases, especially in neoplasms, remain to be elucidated. In the current study, the authors investigated the function of PLEKHO1 in RCC and explored the mechanism in which PLEKHO1 functions.

Materials and methods

Bioinformatic analysis. The raw expression data and clinical data, such as tumour stage and survival status of RCC patients, were downloaded from TCGA, which was searched with the following term: 'KIRC_RNA-seq_HTSeq-Counts' (https://cancergenome.nih.gov/; Tables SI and SII). In the present study, the raw RNA-sequencing (high throughput sequencing-counts) data were arranged and exported using R-project (R version 3.5.0; https://cran.r-project.org/src/base/R-3/), in which 'Edge R', 'gplots' and 'survminer' were used for differential, clustering and survival analyses, respectively. Additionally, co-expression analysis was performed based on the data obtained from cBioPortal for Cancer Genomics using the search term 'Kidney_Kidney Renal Clear Cell Carcinoma (TCGA, Nature 2013)' (http://www.cbioportal.org/) (28,29). Packages were freely accessible from the following sources: 'edgeR': http://www.bioconductor.org/packages/release/bioc/html/edgeR.html; 'gplots': https://cran.r-project.org/web/packages/gplots/; 'survminer': https://cran.rstudio.com/web/packages/survminer/index.html.

Cell lines and cell culture. Human RCC cell lines (Caki-1, 786-O, ACHN, 769-P and OS-RC-2) were obtained from the Cell Type Culture Collection in the Institute of Biochemistry and Cell Biology of the Chinese Academy of Sciences (Shanghai, China). Caki-1 cells were cultured in McCoy's 5A medium (HyClone; GE Healthcare Life Sciences), while 786-O, 769-P and OS-RC-2 cells were cultured in RPMI-1640 medium (HyClone; GE Healthcare Life Sciences), and ACHN cells was cultured in minimum essential media (HyClone; GE Healthcare Life Sciences) at 37˚C with 5% CO_2. All the culture media were supplemented with 10% foetal bovine serum (HyClone; GE Healthcare Life Sciences). 786-O and Caki-1 cell lines were authenticated, and no mycoplasma contamination was identified.

Tissue samples. Paired tumour and para-tumour normal tissues were acquired from 30 patients (19 males and 11 females aging from 35 to 71 years old) diagnosed with RCC who had undergone surgical treatment at the Department of Urology, Cancer Hospital of China Medical University and the Department of Urology, The First Hospital of China Medical University (Shenyang, China) from September 2014 to July 2016. The excised tissue samples were snap-frozen in liquid nitrogen and saved at -80˚C until their use. The current study was approved by the Research Ethics Committee of China Medical University and all patients provided signed written informed consent.

High-throughput cell viability screening. A high-throughput Celigo cytometry system was used to evaluate cell viability as previously described (30,31). In the present study, 786-O cells were chosen as the cell model of RCC and transfected with a short hairpin (sh)RNA to a specific gene or scrambled shRNA (sh-Ctrl; both GeneChem) in the presence of 6 μg/ml polybrene (Sigma-Aldrich; Merck KGaA). To guarantee the shRNA silencing efficiency, three shRNAs [20 μg hU6-MCS-CMV-EGFP (GeneChem)] targeting different sites on each of the 16 candidate genes and the positive control (PC) gene (RNA-binding protein NOB1) were pooled in equal proportions in the packaging viruses. These 16 candidate genes were chosen based on their relevance to the development of RCC after analysing the TCGA dataset: DNA dC->dU-editing enzyme APOBEC-3H, enkurin, α-(1,3)-fucosyltransferase 11, Golgi-associated plant pathogenesis-related protein 1, mixed lineage kinase domain-like protein, nucleoredoxin-like protein 2, opa interacting protein 5, oncoprotein-induced transcript 3 protein, PLAC8-like protein 1, PLEKHO1, protein prune homolog 2, Ras association domain-containing protein 6, spindle and kinetochore-associated protein 3, pachytene checkpoint protein 2 homolog, ubiquitin-conjugating enzyme E2 T and zinc finger protein 320. Two days after transfection, the transfected cells were subjected to cell viability screening, in which a total of 2,000 cells were seeded into each well of 96-well plates and scanned every day using a Celigo Imaging Cytometer equipped with integrated Celigo software (both Nexcelom Bioscience) at a magnification of x100 for 5 days. The fluorescence signal, which was proportional to the live cell number in each well, was quantified automatically and recorded as the cell viability in real time.

Lentivirus construction, and shRNA and siRNA transfection. Lentiviruses carrying shRNAs targeting PLEKHO1 (sh-PLEK;

GeneChem) or scrambled shRNA (sh-Ctrl) were constructed using hU6-MCS-CMV-EGFP. The RCC cells were transfected with sh-PLEK or sh-Ctrl lentivirus ($1x10^8$ TU/ml) at a multiplicity of infection (MOI) of ~5 for 786-O cells or ~10 for Caki-1 cells in the presence of 6 μg/ml polybrene (Sigma-Aldrich; Merck KGaA) according to the manufacturer's protocol. Lentivirus volume used was calculated as the following formula: V = (MOI x N)/$1x10^8$ (V = lentivirus volume, N = cell number). Additionally, siRNAs targeting PLEKHO1 (si-PLEK 1# and si-PLEK 2#) or non-targeting control siRNA (si-Ctrl) were purchased from JTS Scientific. Lipofectamine® 3000 transfection reagent (Invitrogen; Thermo Fisher Scientific, Inc.) was used for siRNA transfection according to the manufacturer's protocol. The efficiency of gene knockdown was identified by reverse transcription-quantitative polymerase chain reaction (RT-qPCR) and western blotting 48 h post-transfection. The targeting sequence of sh-PLEK was 5'-GCTGAGAGACCTGTACAGA-3' and for sh-Ctrl, the sequence was 5'-TTCTCCGAACGTGTCACGT-3'. The sense strand sequence was 5'-AGCUCUACAUCUCUGAGAATT-3' for si-PLEK 1#, 5'-GGACAGCUAUCUUGCCCAUTT-3' for si-PLEK 2# and 5'-UUCUUCGAACGUGUCACGUTT-3' for si-Ctrl.

RNA extraction and RT-qPCR. Total RNA was extracted from cultured cells (Caki-1, 786-O, ACHN, 769-P and OS-RC-2) or tissue samples (RCC tumour and para-tumour tissues) using RNAiso Plus reagent (Takara Biotechnology Co., Ltd.) following the manufacturer's protocol and quantified using a BioDrop Duo UV/VIS spectrophotometer (BioDrop Ltd.). For RT-qPCR analysis, total RNA was converted into cDNA using PrimeScript™ RT Master Mix (Takara Biotechnology Co., Ltd.) according to the manufacturer's protocol. A total of 1 μg cDNA was added to SYBR Premix EX Taq™ (Takara Biotechnology Co., Ltd.). The data were collected on a LightCycler™ 480 II system (Roche Diagnostics) as follows: 50˚C for 2 min, 95˚C for 10 min, and 45 cycles at 95˚C for 10 sec, 60˚C for 30 sec and 72˚C for 45 sec. A melting curve was obtained by increasing the temperature from 40˚C to 97˚C at a rate of 0.4˚C/sec. The results were standardized with the expression level of GAPDH. Relative quantitative analysis was performed with the $2^{-\Delta\Delta Ct}$ method (32). The primer sequences were as follows: PLEKHO1, forward 5'-GAA TCG TGG ATC AAT GCC CTC-3' and reverse 5'-GCG GGA GTG CTG GAT TTT TG-3'; and GAPDH, forward 5'-TGA CTT CAA CAG CGA CAC CCA-3' and reverse 5'-CAC CCT GTT GCT GTA GCC AAA-3'.

Western blot analysis and antibodies. Proteins were extracted from 786-O and Caki-1 cells transfected with shRNAs or siRNAs using 10X (wt/vol) radioimmunoprecipitation assay lysis buffer containing 1 mM phenylmethylsulfonyl fluoride (Beyotime Institute of Biotechnology). The lysate was collected and centrifuged (12,000 x g, 30 min, 4˚C). The supernatants containing proteins were divided and quantified and then denatured at 100˚C for 10 min. A BCA kit (Beyotime Institute of Biotechnology) was used for protein quantification. Equal amounts of protein (30 μg/lane) were separated by SDS-PAGE on 10% gels and subsequently transferred to polyvinylidene fluoride membranes (EMD Millipore). The membranes were blocked with 5% skim milk in Tris-buffered saline with 0.1% Tween (TBST) for 1 h at room temperature and then incubated with primary antibodies at 4˚C overnight. The next day, membranes were washed with TBST three times for 5 min each and then incubated in secondary antibodies at room temperature for 1.5 h. After another three washes with TBST, immunoblot detection was performed using enhanced chemiluminescent reagents (Thermo Fisher Scientific, Inc.). GAPDH was used as an internal reference for total protein detection. The antibodies used were listed as follows: Rabbit anti-PLEKHO1 (cat. no. SAB1401681; 1:200; Sigma-Aldrich, Merck KGaA), mouse anti-GAPDH (cat. no. sc-32233), horseradish peroxidase-conjugated goat anti-mouse IgG (cat. no. sc-2005) horseradish peroxidase-conjugated and goat anti-rabbit IgG (cat. no. sc-2004; all 1:2,000; Santa Cruz Biotechnology, Inc.).

Cell proliferation assay. 786-O and Caki-1 cells were transfected with si-Ctrl and siRNAs (si-PLEK 1# and si-PLEK 2#). Twenty-four hours later, cell proliferation was explored using the Cell Counting Kit 8 (CCK-8) assay (Dojindo Molecular Technologies, Inc.). Briefly, cells were collected 24 h after the siRNA transfection, seeded at a density of 2,000 cells/well into a 96-well plate (150 μl/well) and incubated at 37˚C. At 0, 24, 48, 72 and 96 h, 10 μl of CCK-8 working solution was added into each well and incubated for an additional 1.5 h. The absorbance (optical density) of each well was detected using a microplate reader (Model 680; Bio-Rad Laboratories, Inc.) at a wavelength of 450 nm. For all proliferation assays, three separate experiments were performed.

Cell apoptosis assay. 786-O and Caki-1 cells were cultured in six-well plates and transfected with sh-PLEK and sh-Ctrl as described previously. After 5 days of transfection, cells were collected, washed with D-Hanks (pH 7.2-7.4) pre-cooled at 4˚C and then washed with 1X binding buffer. The centrifuged cells (500 x g for 5 min at room temperature) were resuspended using 200 μl 1X binding buffer with an additional 10 μl Annexin V from the Annexin V Apoptosis Detection kit APC (cat. no. 88-8007; eBioscience; Thermo Fisher Scientific, Inc.). Then, the cells were incubated in the dark for 15 min at room temperature, after which 300 μl 1X binding buffer was added to dilute the solution. Flow cytometry analysis was performed on a Guava® easyCyte HT equipped with InCyte™ 3.1 (both EMD Millipore). Three separate experiments were performed.

Xenografted tumour in nude mice. A total of 20 4-week-old female BALB/c nude mice were purchased from LingChang Science and Technology Ltd. and randomized into two groups: The sh-PLEK (KD) group and the sh-Ctrl (NC) group. $1x10^7$ 786-O cells transfected with sh-PLEK and sh-Ctrl as described above. Two days after transfection, cells were observed under an inverted fluorescence microscope using the light and fluorescence modes at a magnification of x100. 786-O cells without any shRNA transfection (NULL) was used as normal control for cell morphology. Then the shRNA-transfected cells were selected with 3 μg/ml puromycin (Sigma-Aldrich, Merck KGaA). After a stable cell line was established, $1x10^7$ 786-O cells mixed with Matrigel (BD Biosciences) at a ratio of 1:1 were subcutaneously inoculated into the right armpit of nude mice. The body

weight of each mouse and the tumour diameter were measured every week from day 43 after the inoculations of stably transfected cells. The tumour volume (V) was calculated using the following formula: V = 3.14/6 x L x W x W (L, length; W, width). All mice were euthanized with the carbon dioxide method on day 87 with a flow rate set at 25% according to the recommendation of AVMA Guidelines (33). The current study was carried out in strict accordance with the recommendations of the Guide for the Care and Use of Laboratory Animals of the National Institutes of Health (34). The protocol was approved by the Committee on the Ethics of Animal Experiments of China Medical University.

Expression microarrays and Ingenuity Pathway Analysis (IPA). For expression profile analysis after PLEKHO1 knockdown, GeneChip primeview human (cat. no. 901838; Affymetrix; Thermo Fisher Scientific, Inc.) was used. The raw microarray data were arranged with Expression Console™ software (version 1.4; Affymetrix; Thermo Fisher Scientific, Inc.), and differential analysis was performed with the GeneSpring (version 11.5; Agilent Technologies, Inc.). The microarray data were submitted to the NCBI Gene Expression Omnibus public database with the accession code GSE126305 (https://www.ncbi.nlm.nih.gov/geo/query/acc.cgi?acc=GSE126305) and the data analysis was based on IPA (version 43605602; Qiagen, Inc.; www.qiagen.com/ingenuity) (35,36).

Additionally, co-expression analysis was conducted in TCGA dataset to check if PLEKHO1 expression correlated with another protein. In order to diminish the interference raised from the maximum and minimum values, the data of patients whose PLEKHO1 expression levels were in the top 1% when all the patients from TCGA dataset were ranked according to PLEKHO1 mRNA expression were excluded.

Statistical analysis. Statistical analyses were performed with SPSS 21.0 statistical software (IBM Corp.). In cell proliferation, apoptosis and xenograft tumour formation assays, the data with normal distribution are presented as mean ± standard deviation, and the 2-tailed Student's t-test was used to evaluate the significance of differences between two groups. To detect the efficiency of silencing, one-way analysis of variance followed by Dunnett's multiple comparisons tests was used to compare differences among multiple groups. The expression data downloaded from TCGA database with non-normal distribution were presented as the median with the interquartile range and the Mann-Whitney U test was performed to compare groups. The Kaplan-Meier assay and Log-rank test was used for survival analysis. Non-parametric Spearman correlation was used for co-expression analysis. A value of $P<0.05$ was considered statistically significant.

Results

Identifying PLEKHO1 as a potential modulator that promotes cell proliferation in RCC. To explore genes that are potentially relevant to the development of RCC, TCGA database was searched, and the gene expression data derived from 72 RCC and paired para-tumour samples from the same patient were analysed. The gene expression profiles in 69 of the 72 paired samples showed a clear distinction between the cancer and normal control tissues according to the clustering analysis (Fig. 1A). The data of these 69 paired samples were further analysed, and 16 genes that were potentially related to RCC development were screened. These genes were selected on the basis of their high expression levels in tumour samples as well as their research significance based on the literature (Fig. 1A; Table SIII). Next, to screen the potential biological relevance of the 16 candidate genes in RCC, each gene was knocked down in 786-O cells using lentiviruses carrying specific shRNAs, separately. As shown in Fig. 1B and C, only treatment with sh-OIP5, sh-PLEKHO1 or sh-PC, the positive control, markedly inhibited cell proliferation. Although other genes, such as FUT11, were similarly highly expressed in the tumour samples compared with para-tumour samples in TCGA data, treatment with sh-FUT11 did not impact the cell viability of 786-O cells. OIP5 has been shown to be associated with the prognosis of RCC, and reduction of its mRNA expression inhibits cell proliferation in 786-O and Caki-2 cells (37). On the other hand, there have been no reports on the relevance of the PLEKHO1 gene in RCC. Thus, the authors chose to further investigate the functional role of the PLEKHO1 gene in RCC.

Upregulation of PLEKHO1 expression in RCC samples is associated with poor prognosis. It has been reported that PLEKHO1 expression is downregulated in some cancers, such as colon cancer (23), breast cancer (24) and gastric cancer (38). In contrast, in the present study, by researching TCGA data, the authors found that PLEKHO1 expression was upregulated in RCC tissue compared with normal para-tumour tissue (Fig. 2A). To further assess the correlation between PLEKHO1 mRNA expression and clinicopathological characteristics, the 69 patients with primary RCC were divided into two groups by using the median value (raw expression, 3,005) of PLEKHO1 mRNA expression as the cut-off (Fig. 2B). As shown in Fig. 2C, the overall survival rate of patients in the low-PLEKHO1 group was significantly higher than that of patients in the high-PLEKHO1 group. To test this hypothesis, the RNA-seq data of an additional 458 unpaired RCC samples from TCGA database were downloaded. The survival analysis of this dataset containing 527 RCC patients showed a similar result, in which PLEKHO1 expression was increased in tumour tissues compared with 69 normal para-tumour tissues and patients with high PLEKHO1 expression exhibited a worse prognosis compared with those with low PLEKHO1 expression (Fig. 2D and E). Next, the mRNA expression level of PLEKHO1 was detected by RT-qPCR in 30 paired localized RCC and para-tumour normal tissues. As shown in Fig. 2F, PLEKHO1 expression was indeed significantly upregulated in the RCC tissue samples compared with the para-tumour normal tissue samples. These results suggest that the aberrant expression of PLEKHO1 may contribute to the development of RCC.

Reduction of PLEKHO1 mRNA expression inhibits cell proliferation in RCC. To explore the functional role of PLEKHO1 in RCC, several cell models were tested. As shown in Fig. 3A, the mRNA level of PLEKHO1 was high in all five tested cell lines, including 786-O and Caki-1 cells. Then, one shRNA and two siRNAs that specifically target PLEKHO1 were transfected

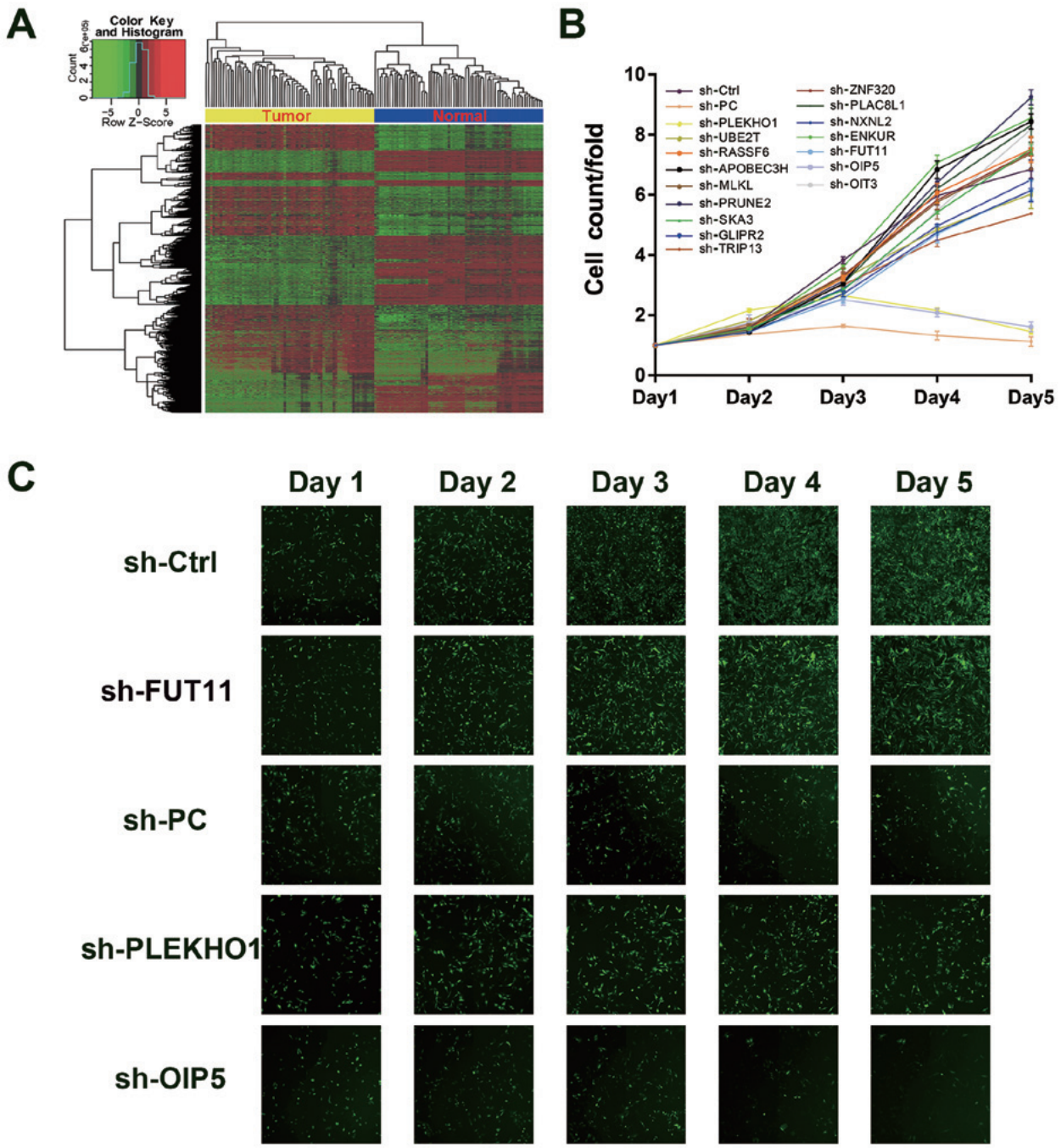

Figure 1. The Cancer Genome Atlas data analysis and high-throughput screening identified PLEKHHO1 as a potential modulator that promotes RCC cell proliferation. (A) Heatmap showing the differentially expressed gene set between paired tumour and para-tumour samples. Each row indicates a gene and each column indicates a patient sample. (B) A total of 16 genes were selected for validation of viability by high-throughput screening. (C) Representative fluorescence images of high-throughput shRNA screening. PLEKHO1, pleckstrin homology domain containing O1; RCC, renal cell carcinoma; sh, short hairpin; sh-Ctrl, negative control shRNA; sh-PC, positive control shRNA targeting NOB1; NOB1, RNA-binding protein NOB1; FUT11, α-(1,3)-fucosyltransferase 11; OIP5, opa interacting protein 5; UBE2T, ubiquitin-conjugating enzyme E2 T; RASSF6, Ras association domain-containing protein 6; APOBEC3H, DNA dC->dU-editing enzyme APOBEC-3H; MLKL, mixed lineage kinase domain-like protein; PRUNE2, protein prune homolog 2; SKA3, spindle and kinetochore-associated protein 3; GLIPR2, Golgi-associated plant pathogenesis-related protein 1; TRIP13, pachytene checkpoint protein 2 homolog; ZNF320, zinc finger protein 320; PLAC8L1, PLAC8-like protein 1; NXNL2, nucleoredoxin-like protein 2; ENKUR, enkurin; OIT3, oncoprotein-induced transcript 3 protein.

into 786-O and Caki-1 cells either permanently or transiently. At 48 h after transfection, both the mRNA and protein levels of PLEKHO1 were effectively reduced by transfection of either the shRNA or siRNAs (Fig. 3B and Fig. S1).

Cells with stable knockdown of PLEKHO1 expression by the shRNA were subjected to a Celigo cell viability analysis. As expected, 786-O and Caki-1 cell proliferation was significantly suppressed by sh-PLEK transfection compared with sh-Ctrl transfection on days 4 and 5 (Figs. 3C and 2D). To further validate the results, a CCK-8 assay was performed with 786-O and Caki-1 cells after treatment with si-Ctrl or two different siRNAs targeting PLEKHO1 (si-PLEK 1# and si-PLEK 2#). Again, treatment with both siRNAs (si-PLEK 1# and si-PLEK 2#) significantly inhibited cell viability in the two

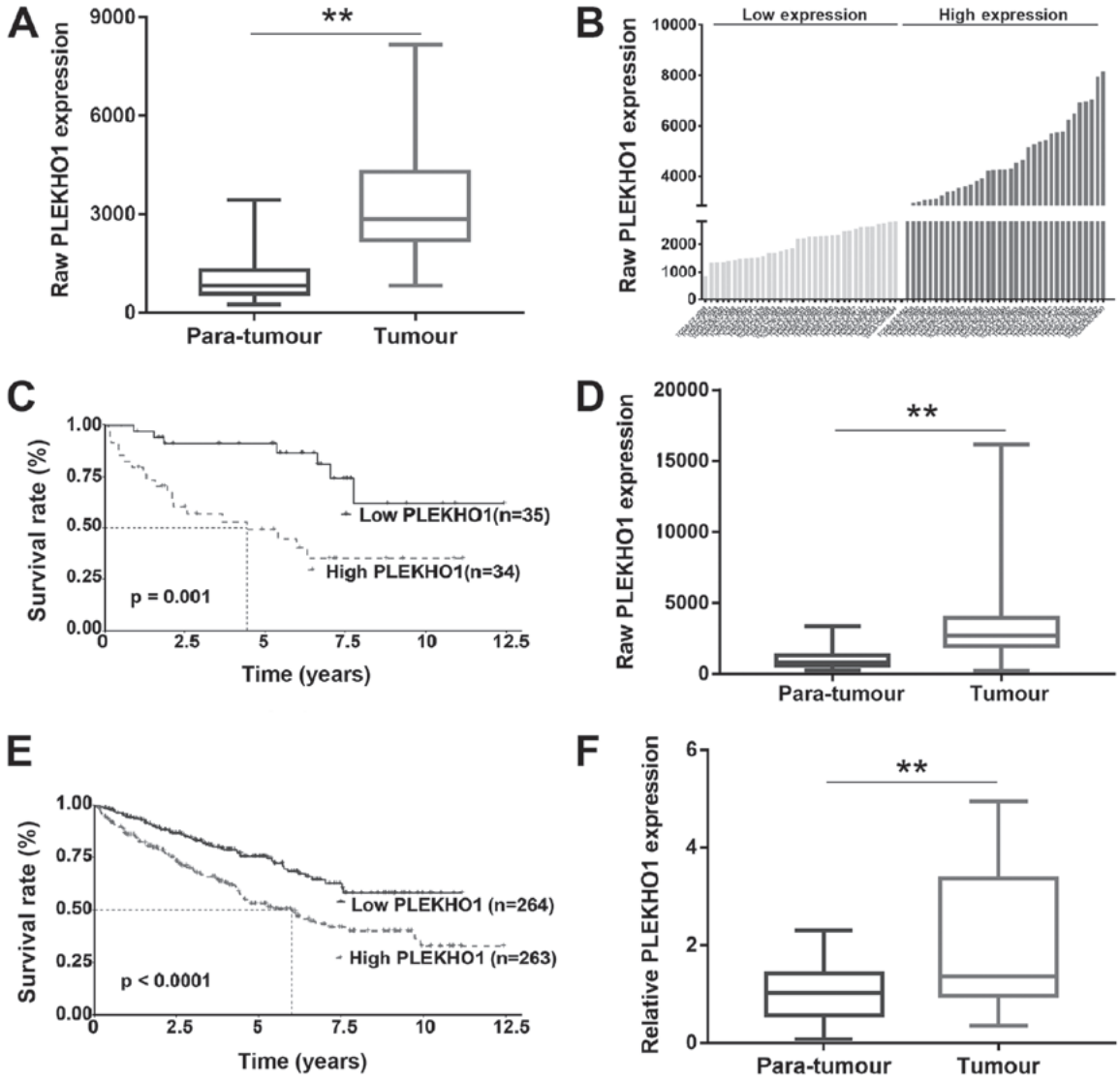

Figure 2. PLEKHO1 is upregulated in RCC tissue and a high level of PLEKHO1 mRNA is potentially associated with a poor clinical prognosis. (A) PLEKHO1 expression RNA-seq data of 69 paired RCC samples in TCGA database. The RNA-seq data are presented as the median with the IQR. (B) A total of 69 patients in TCGA database were classified into two groups according to PLEKHO1 raw expression data, setting the median expression level as the cut-off criteria. (C) Kaplan-Meier overall survival curves according to the PLEKHO1 expression level of 69 RCC samples. (D) PLEKHO1 mRNA expression levels in 527 tumour samples compared with 69 normal para-tumour samples. The data are presented as the median with the IQR. (E) Kaplan-Meier overall survival curves according to the PLEKHO1 expression level of 537 RCC samples (F) PLEKHO1 mRNA expression levels in 30 paired tumour and para-tumour samples. The expression data were presented as the median with the IQR. **P<0.01. IQR, interquartile range. PLEKHO1, pleckstrin homology domain containing O1; TCGA, The Cancer Genome Atlas; seq, sequencing; RCC, renal cell carcinoma; sh, short hairpin; sh-Ctrl, negative control shRNA.

cell lines in comparison with si-Ctrl treatment at 72 and 96 h (Fig. 3E and F). Together, these results suggest that PLEKHO1 may play a role in RCC cell viability.

Downregulation of PLEKHO1 expression induces cell apoptosis. As decreasing the expression level of PLEKHO1 greatly inhibited cell viability, it was hypothesised that PLEKHO1 may affect cell apoptosis in RCC cell lines. Indeed, a flow-cytometric analysis with Annexin V-APC staining showed that the percentage of apoptotic cells in cells transfected with sh-PLEK or sh-Ctrl was 10.36 and 4.25%, respectively, in 786-O cells (Fig. 4A), and 12.05 and 3.33%, respectively, in Caki-1 cells (Fig. 4B). The apoptosis rate was significantly higher in cells transfected with sh-PLEK compared with those transfected with sh-Ctrl. Thus, these results suggest that PLEKHO1 affects the viability of RCC cells at least in part by regulating cell apoptosis.

Reducing the expression level of PLEKHO1 attenuates RCC tumour growth in vivo. To further investigate whether PLEKHO1 affects RCC tumour growth *in vivo*, a xenograft mouse model was used. Compared with the NULL group, cell morphology in the NC and KD groups did not markedly change (Fig. 5A). At the same time, a high transfection efficiency was confirmed with observation under a fluorescence microscope. As shown in Fig. 5B, at the end of the experiment, small tumours formed in only a few mice in the KD group. While in the NC group, xenograft tumours developed in every mouse in which the longest length of these tumours was 19.04 mm (Fig. 5B). Additionally, during the experiment, the tumour growth in the KD group was significantly slower compared with that in the NC group from week 2 to week 7 (Fig. 5C). Accordingly, the tumour weight and tumour volume were both significantly lower in the KD group compared with the

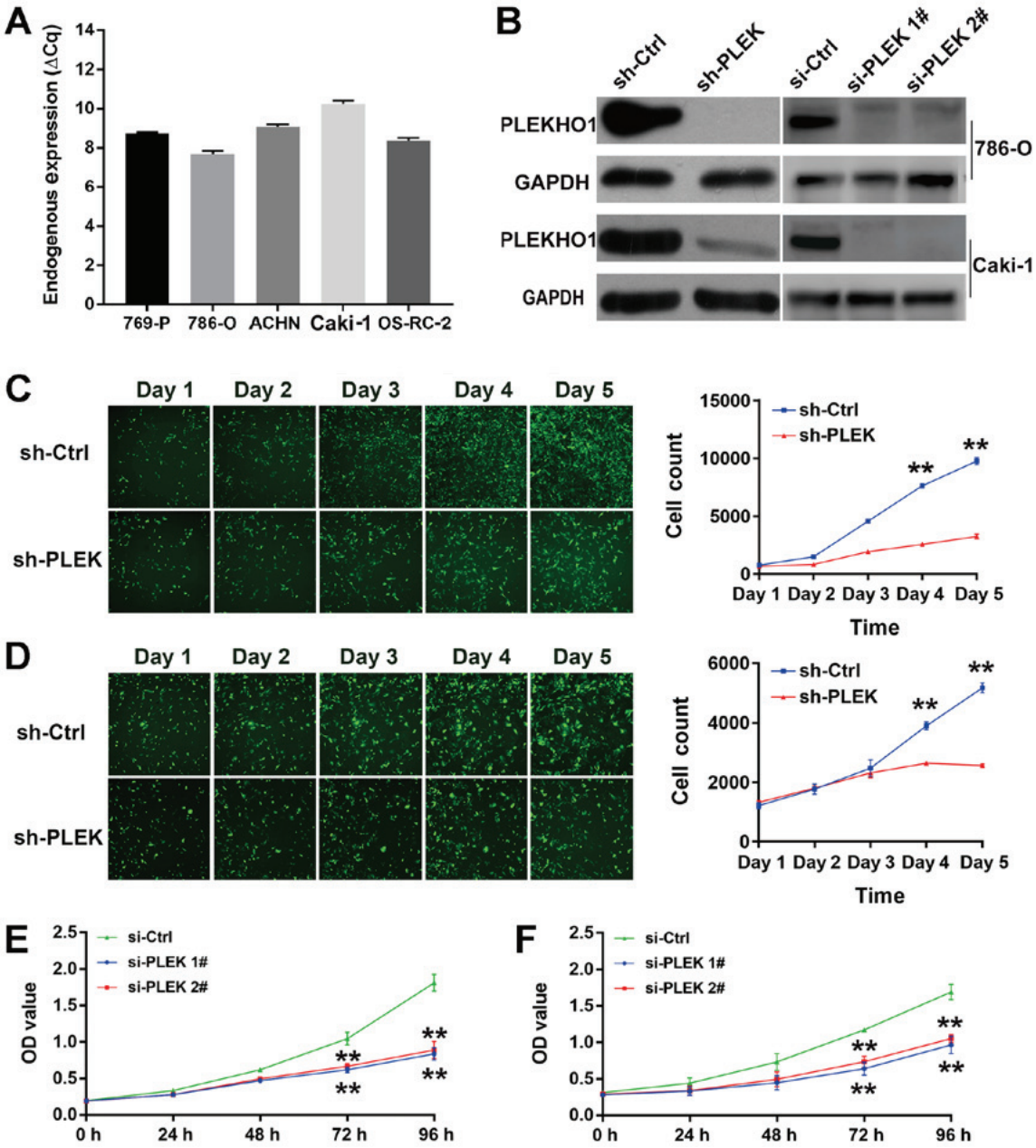

Figure 3. PLEKHO1 downregulation inhibits RCC cell viability. (A) Endogenous PLEKHO1 expression in five RCC cell lines (769-P, 786-O, ACHN, Caki-1, OS-RC-2) was detected by RT-qPCR. (B) The efficacy of shRNA and siRNA in 786-O or Caki-1 cells was detected by western blotting. Fluorescence analysis was used to determine the viability of sh-PLEK-transfected and sh-Ctrl-transfected cancer cells: Representative fluorescence images (left) and the cell growth curve (right) of sh-PLEK and sh-Ctrl (C) 786-O and (D) Caki-1 cells. The cell count is presented as mean ± standard deviation; N=3. **P<0.01 vs. sh-Ctrl. Cell Counting Kit-8 assay showed that the viability of (E) 786-O and (F) Caki-1 cells after the transfection of si-PLEK1#, si-PLEK 2# and si-Ctrl. The OD value is presented as mean ± standard deviation; N=3. **P<0.01 vs. si-Ctrl. RCC, renal cell carcinoma; RT-qPCR, reverse transcription-quantitative polymerase chain reaction; sh, short hairpin; si, small interfering; Ctrl, negative control; PLEKHO1 and PLEK, pleckstrin homology domain containing O1; OD, optical density.

NC group (Fig. 5D and E). These results support the conclusion that PLEKHO1 expression is significantly associated with the proliferative capacity of 786-O cells *in vivo*.

PLEKHO1 may be involved in regulating the serine/threonine-protein kinase hippo and JNK signalling pathways. To further explore the mechanisms underlying the impact of PLEKHO1 on RCC cell viability, total RNA was extracted from 786-O cells with or without knockdown of PLEKHO1 expression and the RNA was subjected to DNA microarray analysis. Upon reducing the expression of PLEKHO1, 196 genes were upregulated, while 403 genes were downregulated (Fig. 6A and Table SIV). Subsequently, upstream IPA showed that PLEKHO1 downregulation impacted the expression of several transcription regulators, including WW domain containing transcription regulator 1 (WWTR1, also known as TAZ; Fig. 6D and Table SV). Additionally, through co-expression analysis on TCGA dataset, it was found that connective tissue growth factor (CTGF), a downstream molecule of TAZ in the Hippo signalling axis, was positively correlated with the expression of PLEKHO1, but negatively correlated with most of the key factors in the Hippo signalling pathway (28,29) (Fig. 6B). Therefore, the authors postulated that PLEKHO1 may function by participating in the Hippo signalling pathway.

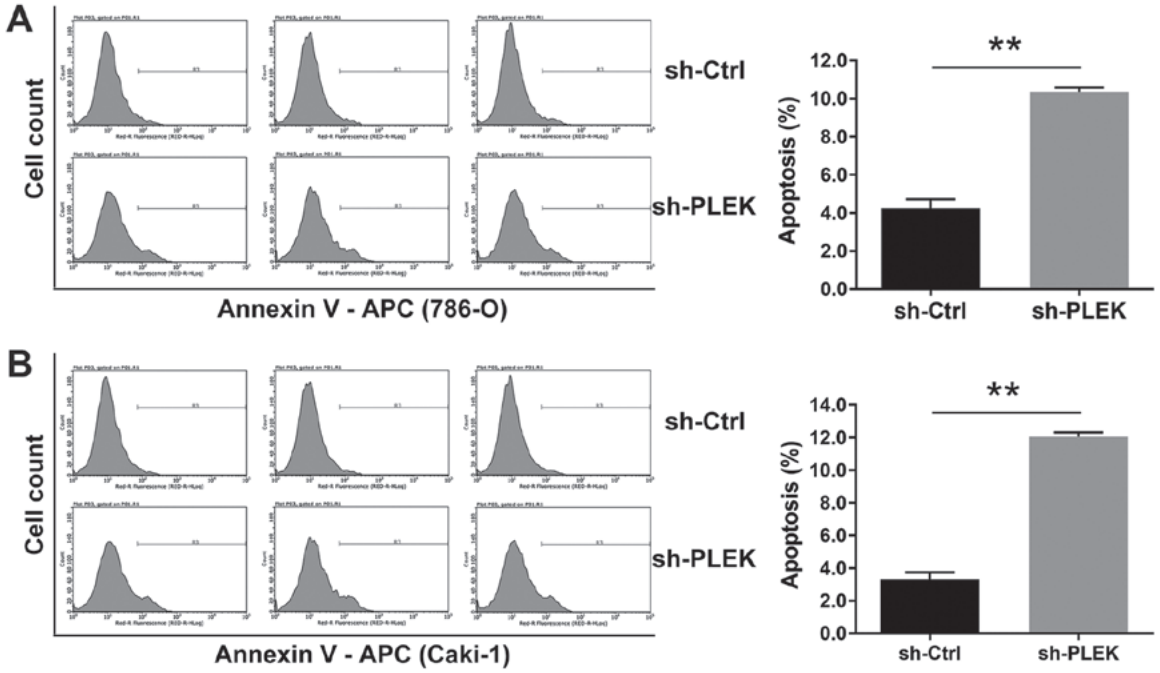

Figure 4. PLEKHO1 interferes with RCC cell apoptosis (A) 786-O and (B) Caki-1 cells transfected with sh-PLEK or sh-Ctrl were stained and analysed by flow cytometry. The percentage of apoptotic cells is presented as mean ± standard deviation; N=3. **P<0.01. RCC, renal cell carcinoma; PLEKHO1 and PLEK, pleckstrin homology domain containing O1; sh, short hairpin.

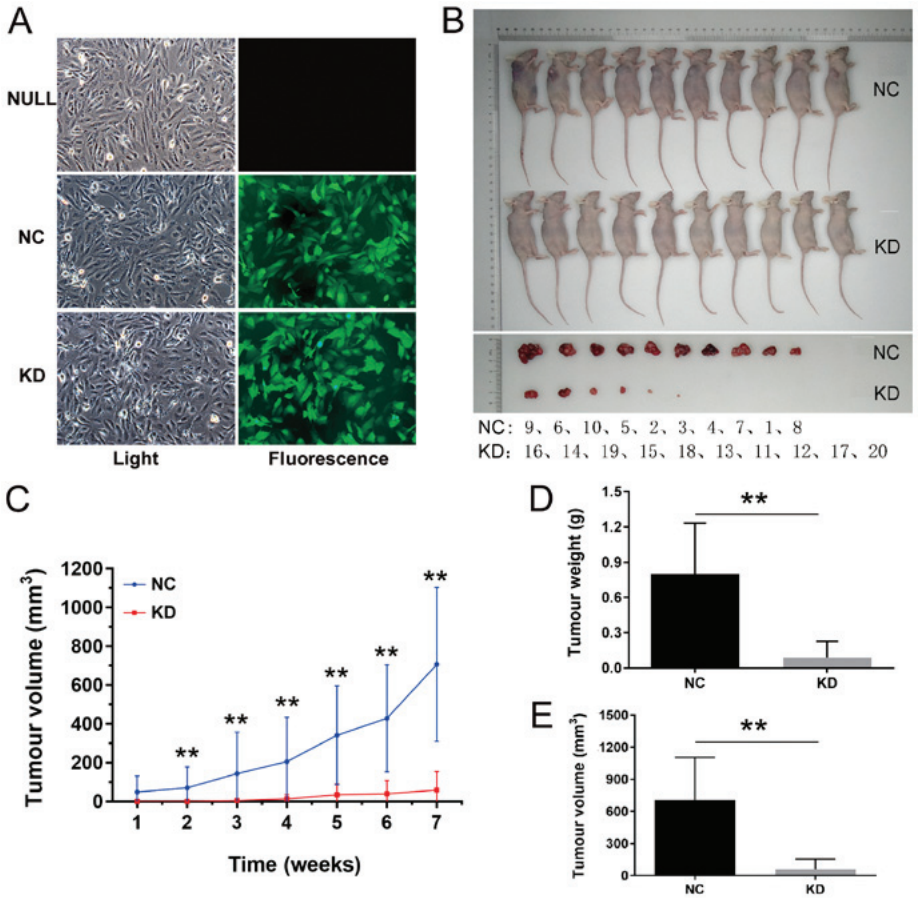

Figure 5. Reduction of PLEKHO1 expression impedes RCC tumour growth *in vivo*. (A) Fluorescence and light microscopy images of 786-O cells infected with KD or NC lentivirus, or NULL. (B) Cells transfected with KD or NC lentivirus were transplanted into 20 nude mice randomized into the KD and NC groups, respectively (N=10). (C) Tumour growth was measured once per week 43 days after transplantation. The tumour growth curve presented as mean ± standard deviation; N=10. The xenografted tumour (D) weight and (E) volume were obtained at 87 days post-transplantation and are displayed as mean ± standard deviation; N=10. **P<0.01. RCC, renal cell carcinoma; PLEKHO1 and PLEK, pleckstrin homology domain containing O1; sh, short hairpin; Ctrl, negative control; NULL, non-transfected cells; KD, sh-PLEK; NC, sh-Ctrl.

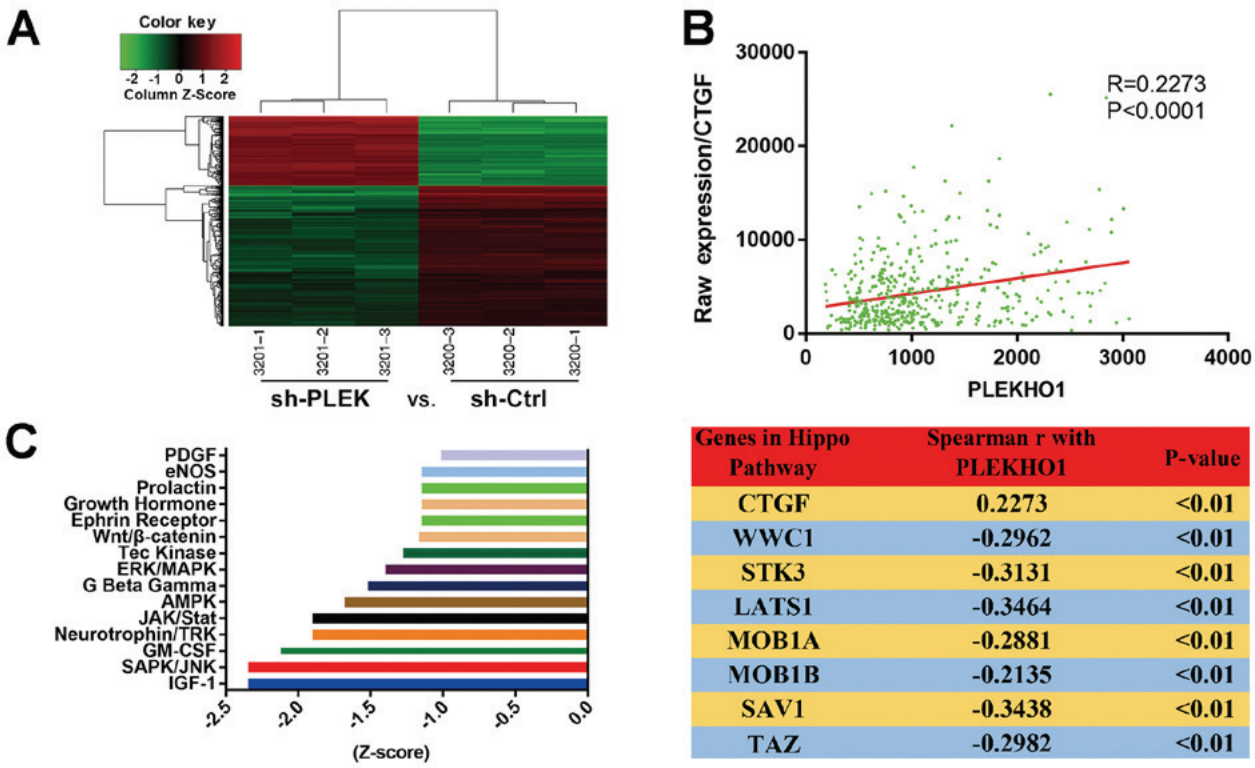

Genes in Hippo Pathway	Spearman r with PLEKHO1	P-value
CTGF	0.2273	<0.01
WWC1	-0.2962	<0.01
STK3	-0.3131	<0.01
LATS1	-0.3464	<0.01
MOB1A	-0.2881	<0.01
MOB1B	-0.2135	<0.01
SAV1	-0.3438	<0.01
TAZ	-0.2982	<0.01

D

Upstream regulator	Expr fold change	Molecule type	Predicted activation state	Activation z-score
TCF7L2	-2.08	transcription regulator	Inhibited	-3.16
NUPR1		transcription regulator	Activated	3.024
KLF2		transcription regulator	Inhibited	-2.9
MEOX2		transcription regulator	Inhibited	-2.53
STAT4		transcription regulator	Activated	2.484
SOX4		transcription regulator	Inhibited	-2.377
E2F1		transcription regulator	Inhibited	-2.358
TP73		transcription regulator	Inhibited	-2.273
WWTR1		transcription regulator	Inhibited	-2.236
PAX6		transcription regulator	Activated	2.236
HMGB1		transcription regulator	Activated	2.22
FOXL2		transcription regulator	Activated	2.216
RUNX2		transcription regulator	Inhibited	-2.2
FOXA1		transcription regulator	Inhibited	-2.176
SRF		transcription regulator	Activated	2.169

Figure 6. PLEKHO1 is involved in the regulation of Hippo and JNK signalling. (A) Heatmap showing the gene expression profiles of sh-PLEK- and sh-Ctrl-transfected 786-O cells. Each row represents a gene and each column represents a sample. Red indicates relative upregulation, whereas green indicates relative downregulation. (B) Co-expression analysis of TCGA data showed the correlation between PLEKHO1 and CTGF (top), and ectopic PLEKHO1 expression correlation with other key factors in the Hippo signalling axis (bottom). Non-parametric Spearman correlation. (C) IPA of canonical pathways. Z-score>0 or Z-score<0 represents 'activated' or 'inactivated', respectively. (D) Upstream analysis of IPA. The top 15 regulators are listed according to the ranked 'activation Z-score'. The activation Z-score exhibits the status of the specific transcription regulators, and the negative or positive value corresponds to 'inhibited' or 'activated', respectively. Hippo, serine/threonine-protein kinase hippo; PLEKHO1, pleckstrin homology domain containing O1; TCGA, The Cancer Genome Atlas; IPA, Ingenuity Pathway Analysis.

In addition to the upstream analysis based on the microarray data, IPA of canonical pathway was performed. Knockdown of PLEKHO1 expression greatly repressed the canonical insulin-like growth factor 1, stress-activated protein kinase (SAPK)/JNK and granulocyte-macrophage colony-stimulating factor signalling pathways (Fig. 6C and Table SVI). As shown in Fig. 6C, the top 15 pathways were highly inclined to be inactivated and JNK was the most canonical and obvious pathway with one of the most negative Z-scores. These results suggest that PLEKHO1 potentially functions through the JNK and Hippo signalling pathways, although further studies are clearly needed.

Discussion

Since PLEKHO1 was first reported, its structural and localization characteristics, and essential functional roles in biological processes have been explored over the past decade (8,9,12-14,17,18). It has been shown that PLEKHO1 expression is downregulated in some cancers and that PLEKHO1 is involved in some key signalling pathways in cancer cells (12,13,23,24,38). For example, Tokuda *et al* (12) reported that PLEKHO1 interacted with Akt through its LZ motif and inhibited PI3K/Akt signalling. Another study found that PLEKHO1 disturbed the endogenous protein level of E3 ubiquitin-protein ligase SMURF1 (Smurf1) by regulating PI3K/Akt/mTOR signalling and therefore promoted the auto-degradation of Smurf1 in colon cancer (23). PLEKHO1 clearly functions as a tumour suppressor gene in these cancers. However, in the present study, aberrant overexpression of PLEKHO1 in RCC tissue samples was observed compared with para-tumour normal kidney tissue samples and found that the downregulation of PLEKHO1 gene expression markedly compromised RCC cell viability. Additionally, reducing PLEKHO1 expression significantly impeded the growth of xenograft tumours in mouse models. Thus, the present results suggest that, at least in RCC, PLEKHO1 promotes cancer development.

It has been reported that PLEKHO1 protein is cleaved into fragments by caspase-3 and that these fragments promote apoptosis through inhibiting the anti-apoptotic activity of c-Jun (13). In contrast, the present study found that PLEKHO1 may protect RCC cells from apoptosis because downregulating the expression of PLEKHO1 induces apoptosis. Thus, it is speculated that PLEKHO1 may function in a context-dependent manner in different cancers through diverse mechanisms.

Furthermore, a gene expression array was performed and it was found that the downregulation of PLEKHO1 impacted the expression of numerous transcription factors, including TAZ. It is known that dephosphorylated TAZ can translocate into the nucleus and function as a co-activator along with its partner AP-1-like transcription factor YAP1 to regulate the expression of CTGF, which is negatively modulated by the Hippo signalling axis (39-41). In mammals, the Hippo signalling pathway plays important roles in organ and cancer development (42). As the main effector of the Hippo pathway, TAZ is destabilized and restricted to the cytoplasm, and therefore loses its transcriptional function when it is phosphorylated by the activated Hippo signalling cascade (43-45). The present co-expression analysis based on TCGA data showed that high expression levels of PLEKHO1 may suppress Hippo signalling and increase endogenous CTGF expression, which is consistent with the result of the microarray analysis. In this context, the authors hypothesized that aberrant PLEKHO1 expression may inhibit the Hippo signalling pathway and activate the activity of TAZ.

Additionally, IPA of canonical pathways showed that PLEKHO1 may interfere with the SAPK/JNK signalling pathway. With sh-PLEK downregulating the level of PLEKHO1 expression, it was found that SAPK/JNK was probably inactivated due to the low Z-score. As a member of the mitogen-activated protein kinase signalling network, the JNK signalling pathway has been proposed to play pivotal roles in cell proliferation, differentiation, death and survival (46). Deregulation of this signalling pathway has been reported in various disease conditions, such as malignancies, diabetes, inflammation and neurodegenerative diseases (46). However, JNK signalling appears to play opposing roles in different cancers. For example, JNK signalling is hyperactivated and promotes cancer development in hepatocellular carcinoma (47,48), lung cancer (49,50), myeloma (51) and skin carcinoma (52). On the other hand, JNK signalling functions as a tumour suppressor in melanoma, lymphoma and chronic myeloid leukaemia (53,54). In the present study, PLEKHO1 knockdown distinctly inhibited RCC cell viability. Simultaneously, microarray analysis showed that PLEKHO1 knockdown potentially restrained the JNK signalling pathway due to the low Z-score. Therefore, the authors of the current study preliminarily hypothesised that JNK functions as a tumour promoter, which mediated PLEKHO1 function and that PLEKHO1 impacts cell viability in RCC partly via regulating the JNK signalling pathway. However, further studies are warranted.

In conclusion, the present study sheds light on the promotive effect of PLEKHO1 on cell viability in RCC, although this protein was speculated to be a tumour suppressor in some other cancers. Thus, further studies are needed to explore the potential of PLEKHO1 as a cancer biomarker as well as a therapeutic target specific for RCC.

Acknowledgements

Not applicable

Funding

This study is partially supported by the National Natural Science Foundation of China (grant nos. 81372766 and 81572532), and the Liaoning 'Climbing' scholarship.

Availability of data and materials

The datasets used and/or analyzed during the current study are available from the corresponding author on reasonable request.

Authors' contributions

ZY and QL conducted the experiments. GZ, CL, QD, and CF participated in data collection and analysis. CK and YZ participated in the design of the study. ZY and YZ participated in the writing of the manuscript and data interpretation. All authors read and approved the final manuscript.

Ethics approval and consent to participate

Experiments using tissue samples from human subjects were approved by the Ethics Committee of China Medical University (Shenyang, China). All participants provided written informed consent for the whole study. Experiments on animals were performed following approval from the Animal Ethical and Welfare Committee of China Medical University.

Patient consent for publication

All participants provided written informed consent for the whole study.

Competing interests

No competing interests.

References

1. Ferlay J, Soerjomataram I, Ervik M, Dikshit R, Eser S, Mathers C, Rebelo M, Parkin DM, Forman D and Bray F (eds): Cancer Incidence and Mortality Worldwide. GLOBOCAN 2012 v1.0. 2013. https://publications.iarc.fr/Databases/Iarc-Cancerbases/GLOBOCAN-2012-Estimated-Cancer-Incidence-Mortality-And-Prevalence-Worldwide-In-2012-V1.0-2012.
2. Ljungberg B, Cowan NC, Hanbury DC, Hora M, Kuczyk MA, Merseburger AS, Patard JJ, Mulders PF and Sinescu IC; European Association of Urology Guideline Group: EAU guidelines on renal cell carcinoma: The 2010 update. Eur Urol 58: 398-406, 2010.
3. Rini BI, Campbell SC and Escudier B: Renal cell carcinoma. Lancet 373: 1119-1132, 2009.
4. Walsh N, Larkin A, Kennedy S, Connolly L, Ballot J, Ooi W, Gullo G, Crown J, Clynes M and O'Driscoll L: Expression of multidrug resistance markers ABCB1 (MDR-1/P-gp) and ABCC1 (MRP-1) in renal cell carcinoma. BMC Urol 9: 6, 2009.
5. Poletto V, Rosti V, Biggiogera M, Guerra G, Moccia F and Porta C: The role of endothelial colony forming cells in kidney cancer's pathogenesis, and in resistance to anti-VEGFR agents and mTOR inhibitors: A speculative review. Crit Rev Oncol Hematol 132: 89-99, 2018.
6. Bedke J, Stühler V, Stenzl A and Brehmer B: Immunotherapy for kidney cancer: *Status quo* and the future. Curr Opin Urol 28: 8-14, 2018.
7. Tomczak K, Czerwińska P and Wiznerowicz M: The Cancer Genome Atlas (TCGA): An immeasurable source of knowledge. Contemp Oncol (Pozn) 19A: A68-A77, 2015.
8. Bosc DG, Graham KC, Saulnier RB, Zhang C, Prober D, Gietz RD and Litchfield DW: Identification and characterization of CKIP-1, a novel pleckstrin homology domain-containing protein that interacts with protein kinase CK2. J Biol Chem 275: 14295-14306, 2000.
9. Safi A, Vandromme M, Caussanel S, Valdacci L, Baas D, Vidal M, Brun G, Schaeffer L and Goillot E: Role for the pleckstrin homology domain-containing protein CKIP-1 in phosphatidylinositol 3-kinase-regulated muscle differentiation. Mol Cell Biol 24: 1245-1255, 2004.
10. Olsten ME, Canton DA, Zhang C, Walton PA and Litchfield DW: The Pleckstrin homology domain of CK2 interacting protein-1 is required for interactions and recruitment of protein kinase CK2 to the plasma membrane. J Biol Chem 279: 42114-42127, 2004.
11. Nie J, Liu L, He F, Fu X, Han W and Zhang L: CKIP-1: A scaffold protein and potential therapeutic target integrating multiple signaling pathways and physiological functions. Ageing Res Rev 12: 276-281, 2013.
12. Tokuda E, Fujita N, Oh-hara T, Sato S, Kurata A, Katayama R, Itoh T, Takenawa T, Miyazono K and Tsuruo T: Casein kinase 2-interacting protein-1, a novel Akt pleckstrin homology domain-interacting protein, down-regulates PI3K/Akt signaling and suppresses tumor growth in vivo. Cancer Res 67: 9666-9676, 2007.
13. Zhang L, Xing G, Tie Y, Tang Y, Tian C, Li L, Sun L, Wei H, Zhu Y and He F: Role for the pleckstrin homology domain-containing protein CKIP-1 in AP-1 regulation and apoptosis. EMBO J 24: 766-778, 2005.
14. Canton DA, Olsten ME, Kim K, Doherty-Kirby A, Lajoie G, Cooper JA and Litchfield DW: The pleckstrin homology domain-containing protein CKIP-1 is involved in regulation of cell morphology and the actin cytoskeleton and interaction with actin capping protein. Mol Cell Biol 25: 3519-3534, 2005.
15. Canton DA, Olsten ME, Niederstrasser H, Cooper JA and Litchfield DW: The role of CKIP-1 in cell morphology depends on its interaction with actin-capping protein. J Biol Chem 281: 36347-36359, 2006.
16. Zhang L, Xia X, Zhang M, Wang Y, Xing G, Yin X, Song L, He F and Zhang L: Integrated analysis of genomics and proteomics reveals that CKIP-1 is a novel macrophage migration regulator. Biochem Biophys Res Commun 436: 382-387, 2013.
17. Zhang L, Wang Y, Xiao F, Wang S, Xing G, Li Y, Yin X, Lu K, Wei R, Fan J, *et al*: CKIP-1 regulates macrophage proliferation by inhibiting TRAF6-mediated Akt activation. Cell Res 24: 742-761, 2014.
18. Lu K, Yin X, Weng T, Xi S, Li L, Xing G, Cheng X, Yang X, Zhang L and He F: Targeting WW domains linker of HECT-type ubiquitin ligase Smurf1 for activation by CKIP-1. Nat Cell Biol 10: 994-1002, 2008.
19. Wang Y, Nie J, Wang Y, Zhang L, Lu K, Xing G, Xie P, He F and Zhang L: CKIP-1 couples Smurf1 ubiquitin ligase with Rpt6 subunit of proteasome to promote substrate degradation. EMBO Rep 13: 1004-1011, 2012.
20. Zhang P, Zhou C, Lu C, Li W, Li W, Jing B, Chen W, Zha Y, Zhang P, Bai C, *et al*: PLEKHO2 is essential for M-CSF-dependent macrophage survival. Cell Signal 37: 115-122, 2017.
21. Zhang G, Guo B, Wu H, Tang T, Zhang BT, Zheng L, He Y, Yang Z, Pan X, Chow H, *et al*: A delivery system targeting bone formation surfaces to facilitate RNAi-based anabolic therapy. Nat Med 18: 307-314, 2012.
22. Koskimaki JE, Rosca EV, Rivera CG, Lee E, Chen W, Pandey NB and Popel AS: Serpin-derived peptides are antiangiogenic and suppress breast tumor xenograft growth. Transl Oncol 5: 92-97, 2012.
23. Nie J, Liu L, Xing G, Zhang M, Wei R, Guo M, Li X, Xie P, Li L, He F, *et al*: CKIP-1 acts as a colonic tumor suppressor by repressing oncogenic Smurf1 synthesis and promoting Smurf1 autodegradation. Oncogene 33: 3677-3687, 2014.
24. Alvarez C, Aravena A, Tapia T, Rozenblum E, Solís L, Corvalán A, Camus M, Alvarez M, Munroe D, Maass A, *et al*: Different Array CGH profiles within hereditary breast cancer tumors associated to BRCA1 expression and overall survival. BMC Cancer 16: 219, 2016.
25. Gong W, Li J, Chen Z, Huang J, Chen Q, Cai W, Liu P and Huang H: Polydatin promotes Nrf2-ARE anti-oxidative pathway through activating CKIP-1 to resist HG-induced up-regulation of FN and ICAM-1 in GMCs and diabetic mice kidneys. Free Radic Biol Med 106: 393-405, 2017.
26. Zhan Y, Xie P, Li D, Li L, Chen J, An W, Zhang L and Zhang C: Deficiency of CKIP-1 aggravates high-fat diet-induced fatty liver in mice. Exp Cell Res 355: 40-46, 2017.
27. Burgess MR, Hwang E, Mroue R, Bielski CM, Wandler AM, Huang BJ, Firestone AJ, Young A, Lacap JA, Crocker L, *et al*: KRAS allelic imbalance enhances fitness and modulates MAP kinase dependence in cancer. Cell 168: 817-829, 2017.
28. Cerami E, Gao J, Dogrusoz U, Gross BE, Sumer SO, Aksoy BA, Jacobsen A, Byrne CJ, Heuer ML, Larsson E, *et al*: The cBio cancer genomics portal: An open platform for exploring multidimensional cancer genomics data. Cancer Discov 2: 401-404, 2012.
29. Gao J, Aksoy BA, Dogrusoz U, Dresdner G, Gross B, Sumer SO, Sun Y, Jacobsen A, Sinha R, Larsson E, *et al*: Integrative analysis of complex cancer genomics and clinical profiles using the cBioPortal. Sci Signal 6: pl1, 2013.
30. Vinci M, Gowan S, Boxall F, Patterson L, Zimmermann M, Court W, Lomas C, Mendiola M, Hardisson D and Eccles SA: Advances in establishment and analysis of three-dimensional tumor spheroid-based functional assays for target validation and drug evaluation. BMC Biol 10: 29, 2012.
31. Feng L, Sun X, Csizmadia E, Han L, Bian S, Murakami T, Wang X, Robson SC and Wu Y: Vascular CD39/ENTPD1 directly promotes tumor cell growth by scavenging extracellular adenosine triphosphate. Neoplasia 13: 206-216, 2011.
32. Livak KJ and Schmittgen TD: Analysis of relative gene expression data using real-time quantitative PCR and the 2(-Delta Delta C(T)) Method. Methods 25: 402-408, 2001.
33. Leary S: AVMA Guidelines for the Euthanasia of Animals: 2013 Edition. 2013. https://www.avma.org/KB/Policies/Documents/euthanasia.pdf.
34. National Research Council: Guide for the Care and Use of Laboratory Animals: Eighth Edition. The National Academies Press, Washington, DC, 2011. https://grants.nih.gov/grants/olaw/Guide-for-the-Care-and-Use-of-Laboratory-Animals.pdf. Ilar Journal 56: NP-NP, 2015. https://doi.org/10.1093/ilar/ilv024.
35. Patel SJ, Sanjana NE, Kishton RJ, Eidizadeh A, Vodnala SK, Cam M, Gartner JJ, Jia L, Steinberg SM, Yamamoto TN, *et al*: Identification of essential genes for cancer immunotherapy. Nature 548: 537-542, 2017.

36. Zhao D, Lu X, Wang G, Lan Z, Liao W, Li J, Liang X, Chen JR, Shah S, Shang X, *et al*: Synthetic essentiality of chromatin remodelling factor CHD1 in PTEN-deficient cancer. Nature 542: 484-488, 2017.
37. Gong M, Xu Y, Dong W, Guo G, Ni W, Wang Y, Wang Y and An R: Expression of Opa interacting protein 5 (OIP5) is associated with tumor stage and prognosis of clear cell renal cell carcinoma. Acta Histochem 115: 810-815, 2013.
38. Ma HW, Xie M, Sun M, Chen TY, Jin RR, Ma TS, Chen QN, Zhang EB, He XZ, De W, *et al*: The pseudogene derived long noncoding RNA DUXAP8 promotes gastric cancer cell proliferation and migration via epigenetically silencing PLEKHO1 expression. Oncotarget 8: 52211-52224, 2016.
39. Zhao B, Ye X, Yu J, Li L, Li W, Li S, Yu J, Lin JD, Wang CY, Chinnaiyan AM, *et al*: TEAD mediates YAP-dependent gene induction and growth control. Genes Dev 22: 1962-1971, 2008.
40. Hao Y, Chun A, Cheung K, Rashidi B and Yang X: Tumor suppressor LATS1 is a negative regulator of oncogene YAP. J Biol Chem 283: 5496-5509, 2008.
41. Zhao B, Li L, Tumaneng K, Wang CY and Guan KL: A coordinated phosphorylation by Lats and CK1 regulates YAP stability through SCF(beta-TRCP). Genes Dev 24: 72-85, 2010.
42. Maugeri-Saccà M and De Maria R: The Hippo pathway in normal development and cancer. Pharmacol Ther 186: 60-72, 2018.
43. Ando T, Charindra D, Shrestha M, Umehara H, Ogawa I, Miyauchi M and Takata T: Tissue inhibitor of metalloproteinase-1 promotes cell proliferation through YAP/TAZ activation in cancer. Oncogene 37: 263-270, 2018.
44. Lei Q-Y, Zhang H, Zhao B, Zha ZY, Bai F, Pei XH, Zhao S, Xiong Y and Guan KL: TAZ promotes cell proliferation and epithelial-mesenchymal transition and is inhibited by the hippo pathway. Mol Cell Biol 28: 2426-2436, 2008.
45. Liu C-Y, Zha Z-Y, Zhou X, Zhang H, Huang W, Zhao D, Li T, Chan SW, Lim CJ, Hong W, *et al*: The hippo tumor pathway promotes TAZ degradation by phosphorylating a phosphodegron and recruiting the SCF{beta}-TrCP E3 ligase. J Biol Chem 285: 37159-37169, 2010.
46. Bubici C and Papa S: JNK signalling in cancer: In need of new, smarter therapeutic targets. Br J Pharmacol 171: 24-37, 2014.
47. Chang Q, Zhang Y, Beezhold KJ, Bhatia D, Zhao H, Chen J, Castranova V, Shi X and Chen F: Sustained JNK1 activation is associated with altered histone H3 methylations in human liver cancer. J Hepatol 50: 323-333, 2009.
48. Barbarulo A, Iansante V, Chaidos A, Naresh K, Rahemtulla A, Franzoso G, Karadimitris A, Haskard DO, Papa S and Bubici C: Poly(ADP-ribose) polymerase family member 14 (PARP14) is a novel effector of the JNK2-dependent pro-survival signal in multiple myeloma. Oncogene 32: 4231-4242, 2013.
49. Takahashi H, Ogata H, Nishigaki R, Broide DH and Karin M: Tobacco smoke promotes lung tumorigenesis by triggering IKKbeta- and JNK1-dependent inflammation. Cancer Cell 17: 89-97, 2010.
50. Luan L, Zhao Y, Xu Z, Jiang G, Zhang X, Fan C, Liu D, Zhao H, Xu K, Wang M, *et al*: Diversin increases the proliferation and invasion ability of non-small-cell lung cancer cells via JNK pathway. Cancer Lett 344: 232-238, 2014.
51. Liu Q, Tao B, Liu G, Chen G, Zhu Q, Yu Y, Yu Y and Xiong H: Thromboxane A2 receptor inhibition suppresses multiple myeloma cell proliferation by inducing p38/c-Jun N-terminal kinase (JNK) mitogen-activated protein kinase (MAPK)-mediated G2/M progression delay and cell apoptosis. J Biol Chem 291: 4779-4792, 2016.
52. Alameda JP, Fernández-Aceñero MJ, Moreno-Maldonado R, Navarro M, Quintana R, Page A, Ramírez A, Bravo A and Casanova ML: CYLD regulates keratinocyte differentiation and skin cancer progression in humans. Cell Death Dis 2: e208, 2011.
53. Gao Y, Tao J, Li MO, Zhang D, Chi H, Henegariu O, Kaech SM, Davis RJ, Flavell RA and Yin Z: JNK1 is essential for $CD8^+$ T cell-mediated tumor immune surveillance. J Immunol 175: 5783-5789, 2005.
54. Xiao X, Jiang K, Xu Y, Peng H, Wang Z, Liu S and Zhang G: (-)-Epigallocatechin-3-gallate induces cell apoptosis in chronic myeloid leukaemia by regulating Bcr/Abl-mediated p38-MAPK/JNK and JAK2/STAT3/AKT signalling pathways. Clin Exp Pharmacol Physiol 46: 126-136, 2019.